Crystal structure and electron density distribution of hydroxyapatite from longgu (Fossilia Ossis Mastodi) in the Kampo medicine prescription

*Yu Kurozumi[1], Junji Yamakawa[1], Kazuki Oguri[3], Kyoko Takahashi[3], Masaya Kawase[2]

1. Okayama University, 2. Nagahama Bio-tec University, 3. Osaka University

longgu (Fossilia Ossis Mastodi) is one of the herbal medicine, and is considered to be a fossil of a large mammal. All longgu used in Japan are imported from China. However, because it is a fossil, there is concern that natural resources will be exhausted. In this study, for the purpose of exploring alternative materials of longgu from a mineralogical point of view, we investigated the change of crystal structure accompanied by longgu in Kampo medicine prescription.
The electron density distribution of the apatite from the longgu samples were investigated by using the noisy XRD data from the laboratory instrument. For the purpose of the noise reduction for the noisy XRD data, the Savitzky-Golay filtering method (Savitzky and Golay, 1964) were applied for the XRD data. Analysis of crystal structure and electron density distribution was carried out by MEM/Rietveld method using RIETAN-FP (Izumi and Momma, 2007).
In this study, medicinal longgu of before use (rawp1), longgu was prescribed with only water (Rp1) and with other natural medicines as Kampo use (Kp1). Symbols, Rpt1and Kpt1 meen three times prescribing Rp1 and Kp1.
The XRD data were obtained by the Rigaku RAD-C Radial X-ray diffraction system. The Cu*K*a radiation with graphite monochromator was used for the measurement. The 2 theta range was from 2 degrees to 120 degrees. The measurement step was 0.02 degrees per step with the 2 seconds of fixed time. The dominant mineral phase for the longgu was identified as hydroxylapatite (HA).
The structural data and the electron density distribution data were required by investigation of the alternative materials and the evaluation of the reusability of the longgu. However, the electron density distribution by the MEM/Rietveld method in this study is considered to be insufficient accuracy for comparison with the electron density distribution by the single crystal method.
Based on the shape of the electron density distribution of PO_4 tetrahedra, it was divided into two groups <rawp1, Rpt1, Kpt1, SHA> and <Rp1, Kp1>. From this, it is considered that the structure is changed by applying Kampo medicine prescription once and that it return to the original structure when it is repeatedly prescribed. It was also confirmed that the XRD pattern of Rp1 has a different peak from that of HA.
Future tasks include increasing the accuracy of measurement of XRD patterns, identifying mineral phases with peaks different from HA of longgu's XRD pattern, and measuring and analyzing longgu of different lots.

Keywords: longgu, Kampo medicine prescription, MEM/Rietveld, hydroxyapatite

Babingtonite with epitaxial hedenbergite whiskers

*Mariko Nagashima[1], Daisuke Hamane[2]

1. Graduate school of Sciences and Technology for Innovation, Yamaguchi University, 2. The institute for Solid State Physics, the University of Tokyo

Babingtonite, $Ca_2Fe^{2+}Fe^{3+}[Si_5O_{14}(OH)]$, is a hydrous pyroxenoid group mineral consisting of chains built from five twisted SiO_4 tetrahedra. It typically occurs in hydrothermally altered zeolite-dominant veins and cavities in basic igneous rocks, and in skarn deposits. Clinopyroxene with diopside-hedenbergite component, $Ca(Mg, Fe^{2+})Si_2O_6$, also occurs in skarns. Although it does commonly not coexist with babingtonite, clinopyroxene whiskers rarely grow on babingtonite. However, their relationship has not been confirmed directly because of the difficulty of simultaneous determination of atomic arrangement in both minerals. In this study, the platy babingtonite (dark green in color) overgrown by clinopyroxene whiskers from two different localities were investigated: (1) Arvigo, Grisons, Switzerland and (2) Kreimbach/Kaulbach, Kaiserslautern, Germany, using transmission electron microscope (TEM) to understand their relationship and formation process. In the both specimens, the boundary between babingtonite and hedenbergite was sharply defined. The relationship of babingtonite (Bab) and hedenbergite (Hd) was determined as Bab[100]//Hd[112] in the Arvigo and Bab[-100]//Hd[1-12] in the Kreimbach/Kaulbach specimen. Diffractions derived from Bab(031) and Hd(02-1) in the Arvigo, and Bab(031) and Hd(021) in the Kreimbach/Kaulbach sample were observed at the identical position. Their topological relationship can be explained by their crystal structures. The reciprocity between babingtonite and hedenbergite is governed by the direction of the SiO_4-tetrahedral chain, and the configuration of octahedra and meets the requirement to associate both structures. A five-periodic chain of babingtonite harmoniously transitions into a two-periodic chain of hedenbergite. The octahedral cluster consisting four octahedra of babingtonite continuously transforms to the octahedral chain in hedenbergite. Therefore, hedenbergite is apparently an epitaxial phase grown on {010} of the platy babingtonite basal. The occurrences of babingtonite with epitaxial hedenbergite imply that they are essentially formed within the babingtonite stability field. At the initial stage, babingtonite formed under high fO_2 and water saturated condition. Subsequently, slight fluctuation, in particular in fO_2, possibly promoted the nucleation of hedenbergite crystals on {010} of pre-existing babingtonite, leading to the epitaxial relation. Hedenbergite whiskers tend to be getting shorter from the centre to the edge of the babingtonite plate in both Arvigo and Kreimbach/Kaulbach specimens, suggesting that the crystal growth of babingtonite continued during hedenbergite formation.

Keywords: babingtonite, TEM, epitaxy

Preliminary srudy on analysis of minerals by laser-induced breakdown specroscopy(LIBS) for application to forensic geology

*Ritsuko Sugita[1]

1. National Research Institute of Police Science

Analysis of minerals by Laser-induced breakdown spectroscopy (LIBS) was preliminary examined for application to forensic investigation of sand grains.
Analysis was performed by LIBS J200 (Applied Spectra Inc.) equipped with CCD broadband detector and 266nm (25mJ) laser. Spot size of laser was 30 or 50 μm and range of analysis was from 190 to 690nm. Samples analyzed were quartz, feldspars, biotite, hornblende, augite, enstatite, olivine and muscovite as major rock-forming minerals, and magnetite, hematite, chromite, siderite, rhodonite, dolomite, and rutile as minerals rich in iron, magnesium, and some other elements. Examination on four iron and two aluminum standard alloys were also performed.
Experimental results showed obviously that number of peaks and their intensities varied widely depending on elements. For example, iron has hundreds of peaks in the range of detection with moderate intensities, but magnesium shows very strong peaks with relatively small number of peaks. This fact indicates that some of elements such as iron will hinder the search of other elements present in small amount, although magnesium as minor element can be detected if the coexisting elements have no overlapping peak.
Comparison of analytical results of major rock-forming minerals showed that peak patterns were different each other. The uniqueness of each result is attributed to elements with strong intensities rather than the type of mineral group. The results of feldspars indicate that it will be possible to estimate concentration of target elements in a previously identified mineral by microscopy or other methods, at least semi-quantitatively level.
Magnetite and hematite provided very similar results, and it was difficult to discriminate each other. Siderite is a mineral also contains a large amount of iron. But the sample used in this examination contained up to 10% of magnesium according to energy-dispersed x-ray analysis, and could be differentiated from magnetite and hematite. Rest of minerals showed different peak patterns from others. Identification of elements in iron-rich minerals required a hard task, and it is expected solving this issue will be an important issue for quantitative analysis.

Keywords: laser-induced breakdown specroscopy(LIBS), forensic geology

Unusual distribution of zeolite in Shirahama Formation, southern Boso Peninsular

*Shigenori Ogihara[1]

1. Graduate School of Science, The University of Tokyo

Zeolite group minerals with unusual occurrence were found from Late Pliocene Shirahama Formation, Cape Nozima and southern Shiramazu, Chikura town, most southern Boso peninsular. Each occurrence of zeolite was carried out the analysis of XRD, XRF, EPMA, carbonate carbon and oxygen isotope.

1. Analcime cemented mud chip (analcime nodule, 60cm x 40cm) in volcanoclastics under the Cape Nozima lighthouse: Mud chip found in volcanoclastic sediment was cemented fine grain analcime and/or calcite. Analcime was very fine grain and could not be observed under the microscope. Some calcite and analcime vein were found around the analcime nodule. Coarse grained analcime, 0.2 mm diameter, was observed in these veins.

2. Coexistane of heulandite and nekoite:Two pumice layers were found under and just above SH tuff, which is the important key bed of the Shirahama Formation. These pumice were altered in tabular heulandite and radiating nekoite. The occurrence of nekoite is first report in Japan. Nekoite was reported from skarun or altered limestone, not reported as diagenetic origin.

Keywords: zeolite, heulandite, analcime, nekoite, erionite

Mineralogy of polygonal serpentine and chrysotile from Kyushu Kurosegawa Belt

*Satomi Enju[1], Seiichiro Uehara[1]

1. Department of Earth and Planetary Sciences, Faculty of Science, Kyushu University

Serpentine minerals are 1:1 type phyllosilicate with ideal composition $Mg_3Si_2O_5(OH)_4$. They take various crystal structure due to the misfit between layers. Chrysotile have cylindrical nanotube like structure and is divided into clinochrysotile (chrysotile-2M_{c1}) and orthochrysotile (chrysotile-2Or_{c1}) by the β angle. Polygonal serpentine (PS) have a unique multi column shaped structure. It can also be divided into two types; “clino-type PS” with XRD pattern similar to clinochrysotile and “ortho-type PS” similar to orthochrysotile (Middleton and Whittaker, 1976; Krstanovic, 1997). Careful observation is required for accurate determination. In our former study, we revealed the types and distribution of polygonal serpentine and chrysotile from Kurosegawa belt, Kyushu, Japan (Enju et al., 2016). The chrysotile and PS from the Kurosegawa belt can be roughly divided into two groups; Ortho-type PS rich type and clinochrysotile-rich type which includes minor orthochrysotile. This biased occurrence is very unique. In this study, we researched the occurrence and chemical composition of PS and chrysotile from Kyushu-Kurosegawa belt to estimate the factors that cause the difference in forming species.

About 300 samples were collected at 28 areas in Kyushu Kurosegawa belt and analysed by XRD (Inoo and Uehara, 2009). Representative samples were chosen considering the result of X-ray diffraction (XRD), and were analysed by electron microprobe analyser (EPMA) and transmission electron microscope (TEM) in Kyushu university ultramicroscopy research center. Two types of TEM samples were prepared; dispersed grains on Cu-grids and ion milled thin sections.

The ortho-PS commonly occur as liner splintery veins, few millimetres in width (Shimotake, Fukami) or irregular veins (Wakayama) in host serpentinites. Clinochrysotile rich specimen occur as thin veins in serpentinites, or as massive aggregates. The clinochrysotile rich samples are Al poor (<0.02 *apfu*), while ortho-type PS rich samples showed various Al contents (0.01-0.09 *apfu*). Al contents of the ortho-type PS differed in localities; Fukami (0.01 *apfu*), Shimotake (0.04-0.05 *apfu*) and Wakayama (0.09 *apfu*). The Fe was mainly divalent estimated from charge balance, and showed no clear difference between the two types (0.03-0.11 *apfu*). The basic properties of ortho-type PS (15 sectored, 200-300nm in general) were common in all samples, but microtexture differed by locality. The chrysotile and PS in Fukami, have smaller diameters with sparse texture, while they occur as incomplete fractures with larger diameter in dense texture in Wakayama. Shimotake was intermediate.

Serpentine veins with different occurrence in Shimotake was observed to estimate the factor that causes different forming species. In Shimotake many splintery serpentine veins occur between spathic serpentinite, pale to apple green, opaque, few millimeters in width, which are all ortho-type PS near endmember. However there is also a wider vein (up to 1 cm) composed of many scale like blocks, yellowish to apple green, opaque to transparent, which is much less common. They are mixture of orthochrysotile and clinochrysotile, and the proportion change through out the vein. The composition of the chrysotile split into two types, Al rich phase (Al 0.02-0.04, Fe 0.04-0.08 *apfu*) and Fe rich phase (Al 0.01-0.02, Fe 0.09-0.12 *apfu*). The Al-rich phase is abundant in orthochrysotile rich specimen and Fe rich phase in clinochrysotile. Also considering that the chemical composition of Al rich phase is close to ortho-PS, the Al content may be responsible for clino-type vs ortho-type, but not for PS vs chrysotile.

Another interesting point is that ortho-PS are always homogeneous, although the composition slightly differs from vein to vein.

Keywords: serpentine, polygonal serpentine, chrysotile, Kyushu Kurosegawa belt

Chemical compositions of tourmaline in Li pegmatite from Sakihama, Myokenzan, Nagatare, and Okueyama, Japan

*Yohei Shirose[1], Seiichiro Uehara[2]

1. The Kyoto University Museum, Kyoto University, 2. Department of Earth and Planetary Sciences, Faculty of Science, Kyushu University

Many pegmatites on a different scale are distributed with a granite in Japan. However, the number of chemically developed pegmatites are limited, such as an Li enriched pegmatite. In this study, a mineralogical approach was performed in the Li pegmatites from Sakihama, Iwate Prefecture, in the Kitakami Belt, Myokenzan, Ibaraki Prefecture, in the Abukuma Belt, Nagatare, Fukuoka Prefecture, in the North Kyushu, and Okueyama, Miyazaki Prefecture, in the Outer Belt of Southwest Japan. In particular, the chemical trends of tourmaline from each locality were discussed.

Though the Li pegmatites have different occurrences and minerals, they contain tourmaline in common. The tourmaline are continuously distributed from the wall zone to the core, changed the occurrence and macroscopic properties (*e.g.*, Shirose and Uehara, 2012; 2013; 2016). The general formula of tourmaline super group minerals is $XY_3Z_6(T_6O_{18})(BO_3)_3V_3W$ (X = Na, Ca, K, Y = Fe^{2+}, Mg, Mn^{2+}, Al, Li, Fe^{3+}, Cr^{3+}, Z = Al, Fe^{3+}, Mg, Cr^{3+}, T = Si, Al, V = OH, O, W = OH, F, O) (Henry *et al.*, 2011). A chemical variation of tourmaline in an Li pegmatite shows increasing (Li + Al) and decreasing Fe^{2+} at Y site from the country rock to the core of the pegmatite, reflecting the chemical development of melts (*e.g.*, Jolliff *et al.*, 1986; Selway *et al.*, 1999).

The scale of Li pegmatites in Nagatare and Myokenzan is larger than the others, and they are chemically developed pegmatites enriched in Cs and Ta in addition to Li. They occur as a dyke without a druse. The tourmaline from Nagatare and Myokenzan are commonly subhedral radial aggregates with small grain diameters. Many of the tourmaline from the core of the pegmatite are altered to muscovite and cloudy.

The Li pegmatite in Sakihama occurs as a dyke with druses. There are intergrowth of tourmaline and quartz, and subhedral to euhedral tourmaline elongated to the core. The latter has a large grain size, and it is up to 10 cm in diameter. For Okueyama, the small Li pegmatite occurs with druse, in REE pegmatite with miarolitic cavities. The tourmaline from Okueyama are subhedral to euhedral crystals. The color of tourmaline in these localities changes from black to deep color and pale color toward the core of the pegmatite.

EPMA analyses show that a $^{Y}(Fe^{2+}) \leftrightarrow ^{Y}$(Li + Al) substitution of tourmaline toward the core of the pegmatite is significant in all pegmatites. However, the tourmaline from Sakihama had $^{Y}Mn^{2+}$ abundantly, and a $^{Y}(Fe^{2+}) \leftrightarrow ^{Y}(Mn^{2+}$ + Li + Al) substitution occurred significantly, followed by a $^{Y}(Mn^{2+}) \leftrightarrow ^{Y}$(Li + Al) substitution. For the trends of $^{Y}Mn^{2+}$ contents in the tourmaline from the four localities, each locality shows different trends of the chemical development (Figure 1). The tourmaline from Okueyama was drastically enriched in $^{Y}Mn^{2+}$, in the Li rich part of the crystals from the druse. For the tourmaline from Nagatare, the contents of $^{Y}Zn^{2+}$ was characteristic (< 0.2 *apfu*). These chemical properties were harmonious with the associated minerals in the pegmatites. Masutomilite generally occurs from Sakihama, and the Zn-bearing tourmaline associates with gahnite. Comparing the trends of chemical compositions of tourmaline enable to obtain the detailed chemical conditions of the pegmatite and host rocks during the formation process.

Keywords: Li pegmatite, tourmaline, Sakihama, Nagatare, Myokenzan, Okueyama

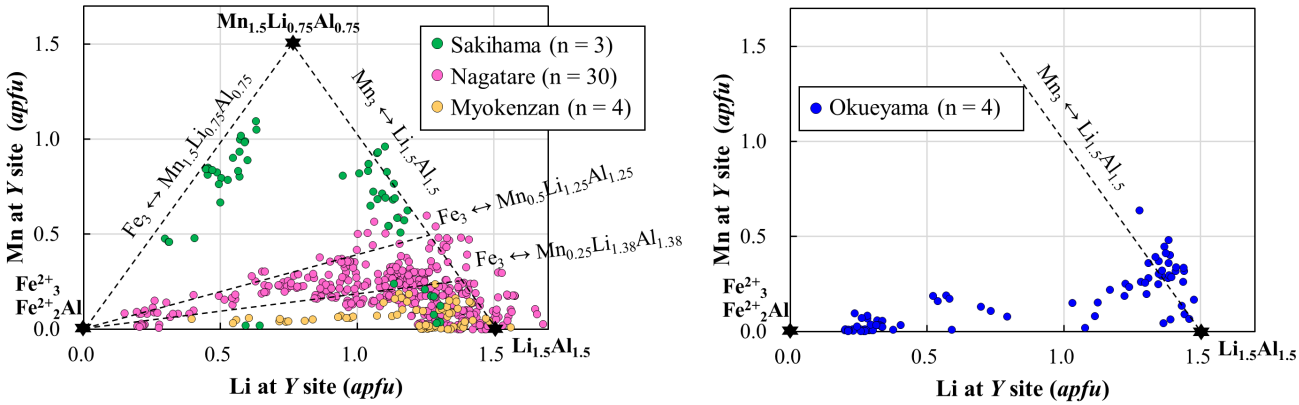

Figure 1 Chemical trends at Y site of the tourmaline from each pegmatite. "n" means the number of specimens. The Li contents were calculated.

A grooved glass surface-plate for making a flat polished surface

*Isoji MIYAGI[1]

1. Geological Survey of Japan, AIST

Recent progress in petrological studies are largely depend on the development of micro-analysis techniques. For micro-analysis such as EPMA, SIMS, and ATR micro-FTIR, the flatness of the polished surface is essential to obtain good analytical results.

Conventional polishing techniques involve final buffing with a cloth, which leads to undesired relief that develops on the polished surface near the boundaries of relatively soft and hard materials; for example, soft glass inclusions in hard quartz phenocrysts, and hard glassy ash particles mounted in soft resin.

A fine-grain abrasive film is more rigid than a cloth and so does not follow the surface differences between different materials. Direct interaction between the flat abrasive film and the flat polishing surface, however, can result in sticking or scratching. Furthermore, a thin fluid film between the polishing surface and the abrasive film can cause the abrasive film to slip.

The newly developed grooved glass surface-plate I present here provides advantages over conventional techniques in terms of making a flat polished surface, even if the sample comprises both relatively hard and soft materials. It allows ideal interaction between the flat polishing surface and an attached abrasive film. The grooves prevent the formation of a film of polishing fluid.

Keywords: EPMA, SIMS, polished sections, ATR micro-FTIR, surface plate

Mineralogical study of lepidolite in Nagatare, Fukuoka Prefecture, Japan

*Takahiro Nogami[1], Seiichiro Uehara[1]

1. kyushu university

1.Introduction
Li pegmatite of Nagatare in Fukuoka prefecture is known to produce various rare element rich minerals, and research on various minerals has been done since 1920’ s. Recently, we conducted a study on elbaite (Shirose ·Uehara, 2013) and reported on changes in the chemical composition of elbaite in the central part from the margin of the pegmatite rock. Especially the elbaite in Nagatarre was characterized by a trace amount of Zn contained compared with other domestic production areas. In this study, we conducted a study on lepidolite which is a representative Li mineral produced in Nagatare, which was insufficiently described. Lepidolite is the name of a solid solution series consisting of trilithionite $K_2(Li_3Al_3)(Si_6Al_2)O_{20}(OH,F)_4$ and polylithionite $K_2(Li_4Al_2)Si_8O_{20}(OH,F)_4$ as an endmember. There is also zinnwaldite series with polylithionite and siderophyllite as an endmember, and this is also a series of mica containing Li. In this study, we aimed to clarify the occurrence and macroscopic characteristics of lepidolite produced in Nagatare, select representative samples, and clarify chemical composition and crystal structure (polytype). Studies of the Muscovite-lepidolite series have been made since long ago, for example Foster (1960) describes the composition and structure change from muscovite to lepidolite, especially the middle part between muscovite and lepidolite is still being discussed.

2. Analysis methods
Samples used in this study were obtained from field survey so far. We classified by macroscopic observation and analyzed using representative samples among them. As a feature of lepidolite in Nagatare, the color is colorless to pink and purple most, and the size of crystals is from 0.1 mm or less to a few centimeters. Symbiotic minerals of lepidolite include quartz, albite, K-feldspar, columbite and the like. For the experiments, identification of mineral species and determination of polytype were carried out by X-ray diffractometer (Rigaku RINT RAPID Ⅱ), and the chemical composition was analyzed using electron probe micro analyser (JEOL JXA-8530F FE-EPMA).

3.Result
Three types of polytype of lepidolite are confirmed, 1*M*, $2M_1$, $2M_2$, and the most common polytype is $2M_1$. Crystals were not confirmed with 1*M* polytype alone, and it was confirmed that $2M_1$ or $2M_2$ was mixed. Fig.1 shows the relationship between chemical analysis values and polytype of each sample in SiO_2 - Al_2O_3 (wt%). From this result, lepidolite is close to the end member of trilithionite, and some samples also contain components of the zinnwaldite series. Considering distinguishing polytype, $2M_2$ lepidolite is closer to polylithionite composition than $2M_1$. Fig.2 shows zoning of lepidolite observed under polarizing microscope. When chemical analysis using EPMA was carried out, Al decreased from the center to the outside, and Si, Li, Mn and F tended to increase.

Keywords: Nagatare, Li pegmatite, lepidolite, polytype, trilithionite, polylithionite

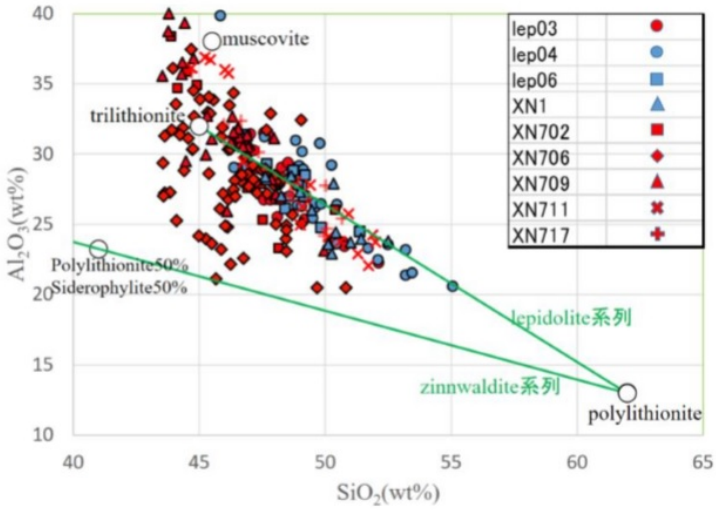

Fig. 1. SiO_2-Al_2O_3(wt%)
red circle shows polytype $2M_1$, blue circle shows polytype $2M_2$.

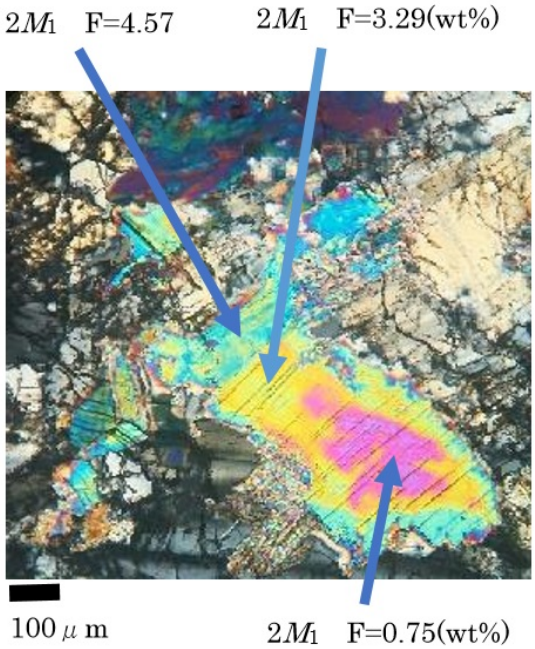

Fig. 2. zoning part of lepidolite (cross polarized)

Mineralogical study of Jadeite-bearing rocks from Kurosegawa zone in Kyushu

*Haruki Inoue[1], Seiichiro Uehara[1]

1. Department of Earth and Planet Sciences, Faculty of Science, Kyushu University.

1. Introduction

The pyroxene group minerals that are the main rock-forming minerals have more than 20 independent species depending on its chemical composition. Jadeite is relatively rare in pyroxene group. Jadeite exists as a jadeitite that occupies more than 90% of jadeite in serpentinite, or included in blueschist and eclogite in serpentinite mélange.

Several jadeite localities in Japan have been reported (Miyajima, 2016). Karakida and Ueda (1983) found albite-omphacite rock including jadeite in Itsuki area, Kumamoto Prefecture and Miyazoe *et al.* (2009) reported *P-T* conditions where the rock was formed at 350 ℃, 500 MPa to 1.08 GPa. Saito and Miyazaki (2006) reported that jadeite-bearing block-shaped metagabbro distributed in serpentinite mélange in Izumi, Yatsushiro city, Kumamoto Prefecture. They mentioned the decomposition reaction of the albite as the formation process of jadeite. Quartz diffused into the surrounding serpentinite via water. In the discussion on jadeite formation process, the decomposition reaction of albite is often cited, but there is a problem that quartz is missing leave process that occurs during the reaction has not been confirmed. Harlow *et al.* (2015) explain that the formation of jadeite caused by the metasomatism with hydrothermal fluid and direct crystallization from hydrothermal fluid, there is a possibility to explain natural occurence of jadeite. In this study, we described the mineralogical description of jadeite-bearing metagabbro in Izumi, Yatsushiro city, Kumamoto Prefecture, and we considered the process of formation of jadeite and omphacite.

2. Geology and sample

The serpentinite mélange of this region consists of Taneyama serpentinite unit, Hakoishi serpentinite unit and Hukami serpentinite unit from the north, distributed in strips in the east-northeast direction (Saito and Miyazaki, 2006). In this study, we investigated jadeite-bearing metagabboro in Hakoishi serpentinite unit reported by Saito and Miyazaki (2006).

3. Experimental method

We observed the thin section by polarized light microscope. Powder XRD analysis carried out by X-ray diffractometer (Bruker AXS, M18XHF22-SRA). Chemical analysis and microstructure observation performed by SEM (JEOL, JSM-7001F) and EPMA (JEOL, JXA-8530F).

4. Results and discussion

The outcrop of the jadeite-bearing flesh metagabbro is dark green. Polished cross section show green or bluish green. The bluish parts contained glaucophane more than the green part. Although most of the observed thin sections contained a pyroxene, jadeite that found with the naked eye was only the white vein with a width of several mm. the other jadeite was scattered as fine grains of about tens of μm. There was also white vein that consist of quartz and potassium feldspar. Fine jadeite grains contained in the vicinity, but it did not coexist with contact with quartz. Powder XRD analysis revealed that constituent minerals in the part without vein were mainly of chlorite, pumpellyite, glaucophane and augite, jadeite was low content compared with these minerals.

Observing the thin section of the rock, fine grains of scattered jadeite gathered with albite and several tens of μm in size. There was no coexistence of quartz. Some also coexisted with potassium feldspar. The part of the vein jadeite consisted of a combination of jadeite and albite in the central part, jadeite and potassium feldspar at the marginal part. Feature rich in Ca, Fe and Mg from the central part to the

marginal part was the same even in the case of scattered jadeite.The chemical composition of the marginal part of the jadeite vein showed the composition that entered the miscibility gap between jadeite and omphacite, possibly forming a very fine lamella.
From above results, it seemed that the quartz reacted with jadeite after it crystallizes out from the hydrothermal fluid, and it became a texture composed of jadeite and albite.

Keywords: Jadeite, Omphacite, Metagabbro, Izumi, Yatsushiro city, Kumamoto Prefecture

Magma process of the Ushikiri-yama granodiorite, north Kyusyu, SW Japan: Implications for formation of middle crust

*Keisuke Eshima[1], Masaaki Owada[1], Teruyoshi Imaoka[1]

1. Graduate School of Sciences and Technology for Innovation, Yamaguchi University

Continental crust comprises mafic lower crust and felsic middle crust in terms of seismic refraction and reflection date (Ansorge et al. 1992). Northern Kyusyu is widely underlain by the granitoid batholiths due to subduction of an oceanic plate during Cretaceous time. The Ushikiri-yama granodiorite intruded at the early stage of igneous activity of the batholiths, and emplaced in the middle crust (Eshima and Owada, 2015). In this study, we address magma processes, emplacement depth, K-Ar mineral ages of the Ushikiri-yama granodiorite, and discuss the formation process of middle crust in the active continental margin.

The Ushikiri-yama granodiorite intrudes limestone, various kinds of metamorphic rocks derived from the Permian accretionary complex. The granodiorite is divided into North and South bodies separated by fine-grained facies granodiorite. It shows hypidomorphic granular texture and consists mainly of plagioclase, biotite, hornblende, quartz, K-feldspar, and trace amounts of euhedral magmatic epidote with Fe^{3+} / (Fe^{3+} + Al^{3+}) values between 25% and 27%. The granodiorite shows flow structure defined by preferred orientation of mafic minerals and plagioclase along the outline of the granodiorite body, and locally contains fine-grained mafic magmatic enclaves (MME).

We estimate the emplacement depth of the Ushikiri-yama granodiorite using the hornblende geobarometer (Schmidt, 1992) with solidus temperature using hornblende-plagioclase geothermometer (Holland and Blundy, 1994). Accordingly, the granodiorite yields emplacement conditions ~720 to 640 ˚C and ~ 0.45 to 0.35 GPa that are equivalent to middle crust conditions. In addition, the granodiorite contains magmatic epidote. It means that the granodiorite magma was produced at the depth of lower crust conditions because the magmatic epidote in granitic magmas can be stable at pressure 0.6-0.8 GPa (Zen and Hammastrom, 1984; Schmidt and Poli, 2004). The emplacement depth of the Cretaceous granitoids from north Kyushu resemble those of the Ushikiri-yama granodiorite, e.g. Itoshima granodiorite (Yada and Owada, 2003). In other words, the granitoid batholiths of north Kyushu would be dominated by the middle crust along the active continental margin during Cretaceous time.

Keywords: middle crust, active continental margin, emplacement depth, magmatic epidote, ushikiri-yama granodiorite

Field occurrence and chemical compositions of granodiorite porphyrites in west coast of the Noko Island, eastern part of northern Kyushu

*Masaki Yuhara[1]

1. Department of Earth System Science, Faculty of Science, Fukuoka University

The granodiorite porphyrite dykes are intruded into metamorphic rocks distributed in west coast of Noko Island, eastern part of northern Kyushu. Karakida (1965) and Karakida et al. (1994) though that they are member of the Kitazaki Tonalite, one of the Cretaceous granitic rocks in northern Kyusyu, based on their features. These dykes include many mafic enclaves.
The granodiorite porphyrites are massive and porphyritic biotite –hornblende granodiorite porphyrite, and composed of mainly plagioclase, hornblende, biotite, quartz, K-feldspar with trace amounts of apatite, titanite, zircon and opaques as accessary minerals. Plagioclase, hornblende, biotite, quartz are phenocryst. Quartz phenocrysts show corroded form. Plagioclase phenocrysts have dusty zone. Mafic enclaves are composed of mainly plagioclase, hornblende, biotite, quartz with trace amounts of apatite, titanite, zircon and opaques as accessary minerals. Plagioclase, hornblende, biotite and trace amounts of quartz are phenocryst. Quartz phenocrysts show corroded form and corona. Plagioclase phenocrysts have dusty zone. These textures of phenocrysts suggest magma mixing.
SiO_2 contents of the granodiorite porphyrite and mafic enclave range from 66.4 to 68.4 and from 60.4 to 61.3 wt.%, respectively. The granodiorite porphyrites have chemical compositions between mafic enclaves and granite porphyrites (Yuhara et al., 2007) intruded into the Kitazaki Tonalite. Most of chemical compositions of mafic enclaves in the granodiorite porphyrite are within that of the Kitazaki Tonalite. But, abundance of MgO, Na_2O and Cr are higher, and Y is lower than that of the Kitazaki Tonalite. The granodiorite porphyrite has been formed by mixing of this magma, which is origin of mafic enclaves, and granite porphyrite magma.

Keywords: granodiorite porphyrite, Kitazaki Tonalite, Noko Island, Cretaceous granitic rocks in northern Kyushu

3D shapes of olivine negative crystals as fluid inclusions in a mantle xenolith from Pinatubo volcano

*Ryuta Nakamura[1], Akira Tsuchiyama[1], Akira Miyake[1], Aki Takigawa[1,2], Akiko Takayama[1], Tsukasa Nakano[3], Kentaro Uesugi[4], Akihisa Takeuchi[4], Tatsuhiko Kawamoto[5]

1. Division of Earth and Planetary Sciences, Kyoto University, 2. The Hakubi Center for Advanced Research, Kyoto University, 3. National Institute of Advanced Industrial Science and Technology, 4. Japan Synchrotron Radiation Research Institute, 5. Institute for Geothermal Sciences, Graduate School of Science, Kyoto University

Olivine is one of the most common minerals in space environments as well as in the Earth. The crystal shapes of olivine may reflect their formation conditions and the anisotropy may affect various physicochemical processes. Crystal shapes are classified into two categories; growth and equilibrium forms. Growth form is reflected by its growth condition while equilibrium form is the form where the sum of the products of surface free energy and surface area is minimum. The surface energies of forsterite, Mg end-member of olivine, were obtained by lattice dynamics [1] and *ab* initio calculation [2] at 0 K in vacuum, and the equilibrium forms were shown.

Last year, we examined the 3D shapes of olivine negative crystals in equilibrated chondrites (LL5-6) [3]. The results show that the degree of annealing can be estimated from the negative crystal shapes and {100) planes, which have high surface energy, develop even on highly annealed negative crystals. However, this is not consistent with the equilibrium from and possibility of absorption of molecules such as H_2O on the surface was discussed. In this study, we observed olivine negative crystals, which are fluid inclusions, in a mantle xenolith to compare with the meteorite samples and to estimate the thermal history of the negative crystals with the mantle origin.

The sample is a harzburgite xenolith in pumice erupted in 1991 by Mt. Pinatubo. Abundant fluid inclusions are present in olivine (Mg#:91-92) grains of the xenolith [4]. Two cylinder-shaped samples 20-30 μm in size containing fluid inclusions were extracted from a polished thin section (#P-3) by using FIB (FEI Quanta 200 3DS). Then, the samples were imaged using imaging microtomography system at beamline BL47XU, SPring-8, Japan with the effective spatial resolution of ~150 nm to obtain their 3D structures. The crystallographic orientations of host olivine crystals were determined with an FE-SEM/EBSD (JEOL 7001F/HKL CHANNEL5). The crystal planes of negative crystals were determined from the CT images together with the EBSD results using the same method as [3].

A void with facets, or negative crystal, ~15 μm in size was present in each sample. Both negative crystals did not have any fluid because a part of the wall of the negative crystal was chipped off during FIB micro-sampling. We observed some evaporation residue, probably NaCl, inside the negative crystals in the CT images. The small chipped portions were manually extrapolated to obtain the whole shapes of the negative crystals. Both negative crystals have well developed {100} planes with high surface free energy as well as {010} planes with low surface free energy.

The above feature is similar to the meteorite samples. In contrast, {001} planes with low surface free energy poorly develop unlike the meteorite samples. It is expected that absorption of water molecules on the surface affects the surface energy. However, relative relation between the surface energies of {100}, {010} and {001} planes is not largely changed according to [1].

The difference in the development of the {001} planes between the Pinatubo sample and meteorite samples is possibly due to the presence of fluid and vapor respectively, in contact with the negative crystal surfaces, or merely fluid and vacuum. The edge of an equilibrium form becomes rounded at high temperatures due to the effect of the entropy of edge free energy. The edges of the Pinatubo samples are sharper than the meteorite samples. The negative crystal shape in the meteorite samples may not be a

strict equilibrium form [3]. We may expect such entropy effect even in the negative crystals that do not have a strict equilibrium form. If this is the case, annealing temperature of the Pinatubo samples is lower than the meteorite samples (1100K).

[1] de Leeuw et al. (2000) Phys. Chem. Minerals, 27: 332. [2] Bruno et al. (2014) JCP, 118:2498. [3] Nakamura et al. (2016) JpGU, PPS12-17 (abstract). [4] Kawamoto et al. (2013) PNAS, 110: 9663.

Keywords: Olivine, negative crystal, xenolith

Bulk water content and hydration of pyroclasts of Asama volcano

Kei Kojima[1], *Hiroaki Sato[2], Keiko Suzuki-Kamata[3], Eiichi Sato[4]

1. Dept Earth Plan Sci, Fac of Science, Kobe Univ, Present address: Insource co., 2. Dept Earth Plan Sci, Grad Sch Sci, Kobe Univ, 3. Dept of Planetary Sci, Graduate School of Sci., Kobe Univ, 4. Inst for Promotion of Higher Education, Kobe Univ

Pre-eruptive andesitic magmas generally contain several weight percent of water, which may vesiculate and degass during eruption. Water content of pyroclasts may bear information of quenching condition of magmas during eruption as well as hydration after the emplacement. We analyzed water contents of pyroclasts of Asama volcano using Karl-Fischer titration method. The age of eruption of the analyzed samples ranges from 20 ka, 13ka, A.D.1108 and A.D.1783. We sieved the sample, selected 4-8 mm clast, split it into two fragments; one used for KFT analyses, and the other half mounted in resin and polished for BSE image and EPMA analyses of glass. Step heating of samples showed 18-35wt% degassing from 0 to 50 C, and gradual degassing up to 500-700 C. Two old samples (Shiraitonotaki pumice fall and Komoro pyroclastic flow) showed ca.50wt% degassing between 200 and 400 C. Totally 159 samples were analyzed by KFT titration. Average water content, standard deviation and number of analyzed samples are 2.60wt%, 0.38, 3 for 20ka (Shiraitonotaki PFa), 2,92, 0.79, 9 for 13ka Tsumagoi PFa, 2.19, 0.51, 27 for 13ka Komoro PFl, 0.50, 0.56, 68 for A.D.1108 Tennin PFa, 0.59, 0.21, 9 for A.D. 1108 Oiwake PFl, 0.46, 0.09, 32 for A.D.1783 Tenmei PFa, 0.65, 0.38, 11 for A.D. 1783 Agatsuma PFl. Even some of the younger eruption products showed higher (>1.0 wt%) water contents. SiO2 contents of matrix glass are 70-71 wt% for 20 ka Shiraitonotaki PFa, 68-77 wt% for 13ka Tsumagoi PFa, 68-80 wt% for 13ka Komoro PFl, 70-77 wt% and 63-67 wt% for A.D.1108 (Tennin PFa and Oiwake PFl, respectively), and 68-72 and 60-73 wt% for A.D.1783 (Tenmei PFa and Agatsuma PFl). There is no correlation between bulk water content and glass SiO2 wt.%. Back scattered electron images of older pyroclasts show brighter glass with darker glass margin of several tens of microns thick. It is inferred that hydration affected the bulk water content of pyroclasts older than 10ka, and limited to those of pyroclasts younger than 1000 years in Asama volcano. Present analyses showed older ejecta (>13000 yrs) have higher bulk water content (average,2.2-2.9wt%) than younger ejecta (<1000 yrs)(average,0.46-0.65 wt%), and bulk water contents are not correlated with mode of eruption, magnitude of eruption, and SiO2 content of glass, suggesting that hydration of glass is extensive for older samples (>10000 yrs) and limited for younger samples (<1000 yrs).

Keywords: pyroclasts, Asama volcano, water content, hydration of glass

Petrology of the Late Cenozoic tholeiitic rock series from Yoneyama area, northern Fossa Magna, Japan

*Masataka Aizawa[1], Satoshi Okamura[1], Toshiro Takahashi[2], (Group) Yoneyama Research Group

1. Hokkaido Education University, Sapporo Campus, 2. Faculty of Science, Niigata University

Late Pliocene-Early Pleistocene volcanic rocks from Yoneyama Formation in northern Fossa Magna consist of basaltic - andesitic pyroclastic rocks and small intrusive rocks, frequently accompanied by Hbl gabbroic xenoliths and Hbl xenocrysts. On the basis of phenocryst assemblage, the volcanic rocks are divided into Ol basalt, Cpx - Opx andesite and Hbl andesite. Nakanodake intrusion in the Yoneyama Formation is composed of inner Cpx - Opx gabbro and outer Hbl andesite, which sometimes contain syenite vein. The volcanic rocks are characterized by high - K and tholeiitic rock series (TH). Two pyroxene geothermometer (Wells, 1977) shows 1100℃ at basalts and 1050℃ at andesites. Ca-amphibole geobarometer (Ernst and Liu, 1998) shows 0.1 - 1.5 GPa at hornblende phenocrysts, 1.1 - 1.5 GPa at hornblende xenocrysts and 0.5 - 0.8 GPa at gabbroic xenoliths, which suggests that hornblende fractionation occurred at depths of lower crust. Hornblende fractionation plays an important role in magma differentiation from basalts to andesites, because of rare earth elements behaviors. H_2O contents calculated by plagioclase hygrometer (Hamada and Fuji, 2007) indicate up to 4.1 wt% at basalts and gabbros, and 3.9 wt% at andesites. We propose that the TH magma from the Yoneyama Formation may have been produced under high water condition.

Keywords: Northern Fossa Magna, Tholeiite rock series, Water content, Ca-amphibole

High-Mg diorite in western Chugoku district: Reagional extension of Cretaceous high-Mg andesite magma

*Shogo Kodama[1], Masaaki Owada[1]

1. Yamaguchi University

Southwest Japan during the Cretaceous was located in the active continental margin along the eastern part of Asian Continent. There are voluminous felsic igneous activities from 105 Ma to 90 Ma. Mafic magmas derived from mantle are assumed as a heat source for the fusion of crust to produce the felsic magmas. The Shimokubara garanite (105 Ma) and Susuma-Nagao granodiorite are exposed in the eastern part of Yamaguchi Prefecture. They geologically occur as the coeval intrusive rocks. The Susuma-Nagao granodiorite is accompanied by dioritic rocks. On the other hand, the Shimokubara granite shows leucocratic and contains porphyritic K-feldspar; thereby both suites show petrographically different character. Therefore, we address the petrological investigation of the Shimokubara granite and Susuma-Nagao granodiorite, and discuss the genetic relationships between granite and diorite to granodiorite magmas.

The Shimokubara granite is characterized by euhedral K-feldspar up to 4 cm. The constituent minerals are Quartz, K-feldspar, Plagioclase and biotite. The Susuma-Nagao granodiorite is medium grained with granodiorite-diorite in compositions. The constituent minerals are plagioclase, hornblende, biotite, quartz with small amounts of K-feldspar.

SiO_2 contents of the Shimokubara granite and Susuma-Nagao granodiorite range from 66-78wt.% and 54-65 wt.%. The Shimokubara granite and Susuma-Nagao granodiorite show the peraluminous and meta-aluminous compositions, respectively, and make a linear trend in the Harker diagrams.

The geological and petrological features of Shimokubara granite and Susuma-Nagao granodiorite are as follows:

(1) Boundary between them is generally unclear and locally including and cutting each other.

(2) Samples collected from such boundary have mixing and mingling texture, e.g., acicular apatite, dusty zoned plagioclase, and quartz ocellar.

(3) Linier trends are shown in the some variation diagrams.

These features suggest that the Shimokubara granite and Susuma-Nagao granodiorite are the coeval intrusive rocks and locally mixed with each other. It means that the Susuma-Nagao granodiorite intruded in this region at the time of 105 Ma, and was chemically modified by the felsic melt from the Shimokubara granite in some places.

The most primitive compositions of the Susuma-Nagao granodiorite have 54 wt.% SiO_2 with up to 6 wt.% MgO. The sample is situated far from the Shimokubara granite and shows free from mixing textures. These geochemical features correlated with those of High-Mg andesite (HMA). In addition, the granodiorite has low- Sr/Y ratio similar to the Sanukitick HMA.

According to the above description, the Susuma-Nagao granodiorite magma would be derived from metasomatized mantle, and penetrate in the crust at 105 Ma. Such mafic magma is caused by the crustal fusion as a heat source and producing felsic melts. Both mafic and felsic magmas are locally mixed with each other.

Keywords: Yamaguchi Prefecture, granodiorite, San-yo belt

Rapid emplacement of granitic magma and formation of upper crust, Cretaceous Hirao granodiorite, North Kyushu, SW Japan

*Yayoi Muraoka[1], Masaaki Owada[1]

1. Yamaguchi University

Cretaceous to Paleogene granitic rocks are widely exposed on the eastern margin of Asian continent. The northern part of Kyushu, Southwest Japan, is underlain by the Cretaceous plutonic and volcanic rocks. The granitic rocks exposed on the eastern part of north Kyushu emplaced into the shallower level of crust accompanied by coeval volcanic rocks. The Hirao granodiorite located in the eastern part of north Kyushu contains magmatic epidote. The magmatic epidote is known that the crystallization is of deeper than middle crust conditions. Sial et al. (2008) reported constraints on depth of emplacement and ascension rate of epidote-bearing magmas. In this study, the author discusses the emplacement process of the Hirao granodiorite magma.

The Hirao granodiorite occurs as a stock with 16 km N-S ×4 km E-W. The granodiorite consists mainly of plagioclase, quartz, K-feldspar, biotite and hornblende with small amounts of epidote. Epidote grains almost show subhedral shapes. In addition, the granodiorite dike occurs in the study area. The granodiorite dike also has mineral assemblage similar to that of the stock.

SiO_2 contents of the Hirao granodiorite range from 62 to 67 wt.%, and increase with decreasing modal values of hornblende. In Sr-Y diagram, the bulk chemical trend can be explained by crystallization of hornblende from parental granodiorite magma. The granodiorite dike shows more evolved conpositions with fractionation of plagioclase in addition to hornblede.

Inferred emplacement P-T conditions are of 0.2-0.4 GPa and 650-700 degrees. These conditions are consistent with contact metamorphic P-T conditions of the Tagawa metamorphic rocks, which are undergone by thermal effect of the Hirao granodiorite magma. These pressure conditions correspond to 6-9 km depth equivalent to upper crust.

Epidote grains in the Hirao granodiorite show subheral shapes with corrosion texture. It means that the epidote underwent corrosion through rapid ascending after crystallized from deeper part of crust. Such rapid ascending system would be caused by a dike (Sial et al., 2008). Therefore, the Hirao granodiorite magma is considered to crystalize epidotes at the deeper part of crust, and emplaced into the upper crust by rapid ascending along the dike.

Keywords: North Kyushu, Granitoids, Magmatic epidote

Petrology of the Itagai gabbroic body, Aomori Prefecture

*Makoto Okazawa[1], Masatsugu Yamamoto[2]

1. Shimane University, 2. Akita University

Itagai gabbroic intrusion, on the border between Akita and Aomori prefectures along shore of Japan Sea, is one of typical tholeiitic bodies consisting of gabbronorite including inverted pigeonite, clinopyroxene, orthopyroxene, plagioclase, magnetite and ilmenite.
Northern end of the Itagai gabbroic body and the Cretaceous Shirakamidake granitic complex are juxtaposed by a fault. But their geological relationship has been unclear. Magnetic susceptibility of both bodies across the fault was mesured and shows increasing in magnetism of Shirakami granitic rocks near the Itagai gabbro. This suggests that the Itagai body is younger than the Shirakami granitic complex.
This body consists of three layers shown by variation of grain size being medium-, coarse-, and fine-grained from south to north. This indicates that Itagai gabbroic body was formed by at least three time's intrusions of magma, which is supported by the different ratio of Sr isotope and mineral chemistry of each layering.
There are more tholeiitic rocks inside and in contact with the Itagai gabbro such as small dykes, Sugozaki quartz diorite and an andecitic intrusion which covered by non-tholeiitic volcanic breccia, forming about 20Ma(Hayashi and Ohguchi,1998). This suggests that tholeiitic magmatism was continued during Paleogene to Early Miocene.

Keywords: gabbro, tholeiite, inverted pigeonite

Magnetic fabric reveals mode of emplacement of Kogarasuyama granodiorite

*Tatsuo Kanamaru[1]

1. Department of Earth & Environmental Sciences, College of Humanities & Sciences, Nihon University

Late Miocene to Pleistocene Higashi-Yamanashi volcano-plutonic complex located in northern part of south Fossa Magna is N-S trending elongated cauldron and is composed of the Kogarasuyama granodiorite and the Konarayama volcanic rocks mainly consisting rhyolitic to dacitic welded tuff. The Kogarasuyama granodiorite intruded into the Konarayama volcanic rocks with sub-vertical contacts. The Kogarasuyama granodiorite showing vertical section of huge dike-like intrusion is cropped out over 1000m in relative height and 25km in length. We carried out anisotropy of magnetic susceptibility measurements for the Kogarasuyama granodiorite. Subvertical magnetic foliations predominantly arrange in a conformable manner to the shape of the body. Sub-horizontal foliations are seen in the inner part of the body. Subhorizontal magnetic lineations are frequently oriented toward elongation trend of the body except at the northern and southern parts of the body. These magnetic fabrics indicate that magmas of the Kogarasuyama granodiorite probably upwelled through subvertical conduit-like regions and successively flowed subhorizontally and that the magma intrusions may have occurred multiply.

Keywords: anisotropy of magnetic susceptibility, Kogarasuyama granodiorite, magnetic fabric, dike, plutonic rock, emplacement

A solidification history of a magma chamber based on textural observations of the Nosappumisaki intrusion, Nemuro, Japan

*Rayko Simura[1]

1. Institute for Materials Research, Tohoku University

Natural rocks are materials in multiphase and multicomponent systems, and they have a lot of information to represent their formation history. We are able to obtain information from the rocks as (1) chemical composition of whole rocks, mineral compositions, and compositional zonings, (2) three-dimensional distribution of particles, shape and size of minerals etc. In order to clarify the history, quantitative analyses are required. However, textural observations and their analyses are not so easier than compositional analyses because of their variety and complexity.
Various methods were conducted on textural analysis of rocks. In most of these studies such images with tracing outer shapes of particles were used [1]. However, the works with manual-handling are time-consuming and sometimes error-prone tasks. Recently, the image analysis using machine learning method as deep learning has been actively developed and applied also on textural analysis of natural rock samples [2]. In order to analyze the texture of the igneous rocks, we need to images with combining the multiple images of the same sample with different angle of polarized light. Previous work of ours introduced the image analysis with using polarization camera. The camera can obtain the image with multiple angle of polarization light in one time. In the camera, polarization films with checkerboard pattern were set on the CCD device, and one picture-cell was obtained by multi-element of CCD[3]. Although the resolution of this camera is enough for strain analysis of glass or plastic, higher resolution is necessary for analyzing the complex texture of igneous rocks. In this study, the system obtaining the images with polarized light were constructed, and the image analysis were conducted for the thin-sections of the Nosappumisaki intrusion, Nemuro, Japan[4]. In the presentation, the result of the analysis will be discussed.
[1]c.f. Morishita R. et al. (1998) Kazan v.5 p.283
[2]c.f. Baykan et al. (2010) Sci. Res. Ess. v.5 p.1243
[3] https://www.photonic-lattice.com (Photonic Lattice, Inc.)
[4]R.Simura and K. Ozawa(2006) J.Pet. v.47 p.1809; R.Simura and K. Ozawa(2011) J.Pet. v.52 p.1887

Keywords: igneous rock texture, polarized light, solidification

Geochemistry and zircon U-Pb dating of volcanic rocks in Mineoka-Setogawa Belt

*Hatsuki ENOMOTO[1], Yuji ICHIYAMA[1], Hisatoshi ITO[2], Akihiro TAMURA[3], Shoji ARAI[3]

1. Department of Earth Sciences, Faculty of Science, Chiba University, 2. Central Research Institute of Electric Power Industry, 3. Department of Earth Sciences, Faculty of Science, Kanazawa University

The Mineoka-Setogawa Belt is distributed from the Boso Peninsula to eastern Shizuoka Prefecture, central Japan and is known as a Paleogene accretionary complex. This belt contains fragments of ultramafic rocks, mafic rocks (gabbro, dolerite, basalt), and pelagic and terrigenous sedimentary rocks, which are interpreted as an ophiolite mélange. However, it has been still controversial for the origin of this ophiolitic mélange. In this study, we aimed to focus on the relationship between the geochemical composition and radiometric ages of the volcanic rocks of the Mineoka-Setogawa Belt.
The collected samples are subdivided into three types on the basis of the mineral assemblage. Type 1 consists mainly of plagioclase and clinopyroxene. Type 2 and 3 are characterized by the presence of biotite + apatite and quartz in addition to plagioclase and clinopyroxene, respectively. The whole-rock compositions of Type 1 and 3 are similar to those of mid-ocean ridge basalt (MORB) and island-arc tholeiite, respectively. On the other hand, the composition of Type 2 is similar to those of intra-plate alkaline basalt. The rare earth element (REE) patterns of Type 1 and 3 exhibit slight depletion in light REE. The REE patterns of Type2 are characterized by light REE-enrichment and heavy REE-depletion. We tried to determine the zircon U-Pb dating from five coarse-grained doleritic samples and succeeded to collect zircon grains from a Type 3 sample. The zircon U-Pb dating using LA-ICP-MS resulted in 18.51±0.82 Ma. This age is close to the whole-rock K-Ar ages (5.8Ma and 15.6Ma) for andesitic tuff breccia by Mori et al. (2011).
The whole-rock K-Ar ages obtained in the previous studies show a wide range from 19 to 42 Ma, which is probable to be affected by secondary alteration. Hirano et al. (2003) and Mori et al. (2011) reported Ar-Ar plateau ages (about 50 Ma and 80 Ma) from MORB-like basalts equivalent to Type1. These ages are probably reliable because they are almost consistent with those of microfossils in pelagic sediments. The compositional difference between these MORB-type basalts of about 50 Ma and 80 Ma is unclear, but, at least, the 80 Ma MORB-type basalt formed in the Pacific Ocean because any other oceanic plate formed in this period is not known. On the other hand, there are several likely candidates for the origin of the 50 Ma MORB-type basalt: Pacific Ocean MORB, West Philippine Sea back-arc basin basalt (BABB), and Mariana fore-arc basalt (FAB). Comparing the Type 1 basalt with these candidates using the REE pattern and the Ti-V diagram of Shervais (1982), the Mineoka-Setogawa MORB-like basalt (Type 1) is similar to Pacific Ocean MORB and West Philippine Sea BABB, but not to Mariana FAB. Hirano et al. (2003) and Mori et al. (2011) also reported Ar-Ar plateau age (25.5 Ma) and Ar-Ar isochron age (19.6 Ma) for intra-plate alkaline basalts equivalent to Type 2. These ages are supported by the occurrence of intra-plate basalt erupted at the same time as Early Miocene mudstone (Sugiyama, 1995). Around this time, the Shikoku Basin had been already formed. We compared the Mineoka-Setogawa Belt Type 2 basalt with alkaline basalts from seamounts on the Pacific Plate and Shikoku Basin. As a result, The Type 2 basalt is closely similar to the former in the point of view of significant enrichment in LREE and depletion in HREE. The island-arc tholeiite (Type 3) formed in around 19 Ma was probably generated by the early volcanism in the Izu-Bonin-Mariana Arc after the Shikoku Basin formation.

Keywords: Mineoka-Setogawa Belt, Paleogene accretionary complex, ophiolite, zircon U-Pb dating

Petrological study on the mafic igneous enclaves in the Miocene Miuchi granitoid pluton, southern Ehime Prefecture

megumi Shiota[2], Fuma Yamasaki[2], *Satoshi SAITO[1]

1. Graduate School of Science and Engineering, Ehime University, 2. Faculty of Science, Ehime University

Mafic igneous enclaves with sub-angular shape are commonly occurred in the Miocene Miuchi granitoid pluton, southern Ehime Prefecture. The mafic enclaves (61-64 wt.% SiO_2, 0.5-2.6 wt.% K_2O) are composed mainly of plagioclase, biotite, quartz and opaque minerals. Acicular apatites are common in the mafic enclaves. Intergrowth texture of biotite and quartz/plagioclase are locally observed in the biotite-rich mafic enclaves. K_2O contents of the mafic enclaves increase with increasing SiO_2. Orthopyroxene, locally surronded by biotite, occurs in the mafic enclave with the lowest SiO_2 and K_2O contents. Biotite-rich reaction rim is observed between the orthopyroxene-bearing mafic enclave and host granite. The host granite samples surrounding the mafic enclave are relatively depleted in the K-feldspar (granodiorite in composition) compared to the dominant rock type of the Miuchi granitoid pluton (monzogranite - granite in composition) (67-78 wt.% SiO_2, 3.3-6.5 wt.% K_2O). The petrographic and geochemical characteristics of the mafic enclaves are suggestive of interaction with host granite magmas through hydration crystallization reaction: hydrous granitic melt + pyroxene + Fe-Ti oxides ±calcic plagioclase = biotite + quartz ±sodic plagioclase (e.g. Bard et al. 2005, J. Geol.).

Keywords: Miuchi pluton, Granitoid, Mafic igneous enclave

